Physical ageing effect on water uptake and adhesion of epoxy coatings by EIS and the blister test

Ismail Kada, Dao Trinh, Stéphanie Mallarino, Sébastien Touzain

Physical ageing effect on water uptake and adhesion of epoxy coatings by EIS and the Blister test

Ismail Kada, Dao Trinh, Stéphanie Mallarino, Sébastien Touzain*

Laboratoire des Sciences de l'Ingénieur pour l'Environnement, LaSIE UMR 7356 CNRS, La Rochelle Université, Avenue Michel Crépeau, 17000 La Rochelle, France

*Corresponding Author: sebastien.touzain@univ-lr.fr

Abstract

In a previous work, it was shown that the physical ageing of organic coatings had a strong effect onto the water uptake process, leading to lower water uptake values at saturation. The service life of an organic coating can be related to the water content at saturation, that may induce corrosion of the substrate, but also to the adhesion that prevents direct contact between the substrate and the aggressive environment. In this work, the effect of physical ageing onto water uptake and adhesion of epoxy coatings onto aluminium is then investigated.

A model epoxy coating (DGEBA/Jeffamine230) was applied onto aluminium panels and fully cured using adequate thermal cycles. Different amounts of physical ageing were created by controlling the cooling of the systems and measured thanks to modulated differential scanning calorimetry (MDSC). The coated panels were then immersed in sodium chloride solution ($30 g.L^{-1}$) at different ageing temperatures. The water uptake was calculated using EIS thanks to the Brasher and Kingsbury relation and the diffusion coefficients were evaluated using the dual-Fick diffusion model.

For different values of physical ageing and different amounts of water uptake, the adhesion was evaluated using the blister test method. The obtained results allow to discuss the effect of physical ageing onto the water uptake content and the adhesion of organic coatings.

Keywords

Physical ageing; Water uptake; Adhesion; Organic coatings; EIS; Blister test.

1. Introduction

Corrosion protection can be achieved through a variety of means and one cost-effective option is the use of epoxy-based coatings. However, these coatings may be subject to degradation in environments characterized by high humidity, salt content, oxygenation, and sunlight exposure. This leads to a weakening of the physical-chemical and mechanical properties and therefore to a degradation of the coatings [1–5]. It is then crucial to predict their lifetime through a better understanding of the phenomena that take place in the polymer, especially when they are submitted to "physical ageing". This ageing phenomenon was described in details by Struik [6–8] and is due to structural relaxations of the polymer chains below the glass temperature (Tg) as a way to tend to an equilibrium state. Indeed, when polymers are cured above Tg and the temperature is cooled down below Tg, the polymer network is in a nonequilibrium state because the polymer chains do not have enough time during cooling to reach equilibrium. This leads to high values of volume, enthalpy and entropy and it means that the polymer network tends to recover an equilibrium state during its service life, leading in particular to a decrease of the free volume. Physical ageing (P.A.) of glassy polymers, as defined by Struik (and adopted in this paper), is then only due to structural relaxations which are in relation with non-null molecular mobility of polymer chains below Tg. It is then different from network changes due to an increase of the curing degree / small molecules absorption or to external factors (mechanical stresses, chemical degradation, thermal degradation, …).

Mechanical, thermodynamic, and physical characteristics of epoxies are then specifically affected by P.A. in a way that drastically modifies the overall behavior of these polymers [9,10], which impacts performance and durability. Researchers have combined this phenomenon with water absorption into coatings, which is recognized as an essential problem [4] since water penetration is the first stage in their degradation process. Some authors report that physical ageing has a low influence on water diffusion in polymer, e.g Akele et al. [11] who studied the effect of physical ageing and water sorption in polycarbonates. Other studies showed that the quantity of water absorbed in polymers at equilibrium is mostly influenced by the polymer's structure [12–14]. This was clearly seen by Kong [10] in a study concerning physical ageing in neat epoxy and composites, where he demonstrated that the diffusion rate and water absorption at saturation were reduced in presence of physical ageing. More recently, a number of noteworthy studies, relating physical ageing and water uptake, have been published. Starkova et al. [15] studied the anomalous water absorption for a neat epoxy

and epoxy/carbon composites and they found that after re-drying of their epoxy systems, thermal and thermomechanical properties were conserved or improved, suggesting the presence of physical ageing in the polymer. Le Guen-Geffroy et al. in 2019 [16] investigated the relationship between physical ageing and plasticization in amine-epoxies hygrothermally aged in saltwater and discovered that physical ageing occurs more faster in a wet environment than in a dry environment. Moreover, the same researchers found later [17] that attention must be taken to distinguish property modifications caused by water penetration from those caused by physical ageing related to polymer chain reorganization. The last one tends to decrease fracture toughness. The mechanism of water absorption is slow at temperatures far below the glass transition temperature (Tg), but when temperatures are elevated to speed it, physical ageing is also accelerated. It is then clear that water diffusion processes and physical ageing can have reciprocal influences which have to be better explained.

Once water has diffused within the coating, it reaches the interface and can affect adhesion to the substrate so the durability of the coating/metal interface. Many methods have been developed (e.g. ISO 2409, ISO 4624) to evaluate the adhesion of organic coatings but very often, they are non-quantitative, non-reproducible, performed in dry conditions, or overestimate adhesion as a result of energy consumption by other phenomena, such as plastic deformation [18]. The blister test (BT) was proposed in 1961 by Dannenberg [19]. The principle is to inject a liquid at the coating/substrate interface in such a way the coating is detached from the substrate in form of a blister. Pressure and volume of the injected liquid are measured and used to compute the work needed for the blister formation. In order to inject the liquid at the coating/metal interface, a hole is drilled through the substrate before application of the coating. The main advantage of the BT is that it provides a measure of the normalized energy needed to initiate/ propagate a crack at the substrate/polymer interface [20] and it can be performed in presence or not of water.

The aim of this work is to investigate the effect of physical ageing onto the water absorption characteristics and adhesion of epoxy coatings applied onto aluminum substrates. Different amounts of physical ageing (P.A.) in epoxy networks were obtained by varying the cooling procedure and were measured by modulated differential scanning calorimetry (MDSC). Electrochemical impedance spectroscopy (EIS) was used to measure water uptake and the blister test was used with dry and water-saturated coatings.

2. Experimental

2.1. Materials

The epoxy coatings were prepared from Diglycidyl Ether of Bisphenol A (DGEBA D.E.R.™ 332) cured with an amine hardener Jeffamine D-230 (ref. 9046-10-0). All materials were obtained from Sigma Aldrich and were used without further purification. The DGEBA resin was mixed with stoichiometric amounts of the amine hardener at room temperature and then degassed under vacuum to remove air bubbles.

For coating samples, the mixture was deposited onto A-46 aluminium Q-panels (0.6 x 102 x 152 mm), cleaned with acetone and ultrasound. For blister test samples, the resin was applied onto A-46 aluminium discs, with a 6mm diameter hole in the center, which were first abraded using 2400 silicon carbide papers grits, and then cleaned with acetone. The hole has to be closed so the liquid DGEBA/JeffamineD-230 resin cannot go into the hole during curing. So, when the blister test is performed, there is no stress concentration at the hole circumference which might introduce cohesive failure of the coating within the thickness, instead of adhesive failure at the coating/interface. A sticker was used to block the hole instead of an inert blanking plug. The coating thickness above the sticker is then lower than that above the metal interface so cohesive cracks can be initiate parallel to the surface if adhesion is stronger than cohesion. Hence, cohesive and/or adhesive failures can be observed with the same test procedure. A large 24mm diameter sticker was used to avoid edge effects of the 6mm diameter hole drilled into the substrate.

All specimens were inserted in a mould constituted by two aluminium plates covered by Teflon sheets and separated by thick spacers to get the desired thickness. Then, the samples were cured in an oven till 120 °C, which is a temperature above Tg, using a curing protocol in order to obtain a homogeneous fully cured network, as presented elsewhere [21]. Finally, the dry film thickness for coatings samples was about 120 ± 10 µm while that of the blister samples was about 350 ± 20 µm (measured by an Elcometer 311 Gauge Thickness).

Three different epoxy networks with different physical ageing amounts were obtained thanks to three different cooling processes. The first process consisted of placing the mould containing the sample between two fans blowing air for a fast cooling just after the curing [21]. Then, the temperature was rapidly reduced below Tg, preventing physical ageing of the organic coating (systems without physical ageing). The second and third processes were to

leave the samples-containing mould in the oven and to apply two cooling plateaux: 1 hour at 88°C (Tg-5 °C) for a system with intermediate physical ageing and 76 hours at 73°C (Tg-20 °C) for a system with a maximum of physical ageing were applied for the second and the third cooling processes respectively. This allowed the temperature to be gradually reduced and the coated panel to be kept at temperatures below Tg for different periods of time, causing different amounts of physical ageing. The time/temperature couples were defined from an initial study (not presented here). The cured specimens were stored in a desiccator to prevent moisture ingress.

2.2. Techniques

2.2.1. Modulated Differential Scanning Calorimetry (MDSC)

The DSC curves were obtained using about 11 ± 1 mg of epoxy material on a DSC Q-2000 instrument (TA Instruments) with MDSC as mode of operation to evaluate the glass transition temperature Tg at a dry state and to quantify the physical ageing. A temperature modulation of ±0.48 °C every 60 seconds was overlaid on a temperature scan (2 °C/min) from 20 °C to 140 °C, approximately 50 °C above the Tg. The cooling ramp was done with the same temperature scan rate. All measurements were carried out under a nitrogen atmosphere with a flow of 50 ml/min. Several identical specimens were tested for reproducibility.

2.2.2. FT-IR analysis

Fourier transform infrared (FTIR) analyses of materials were carried out to characterize the different functional groups of the coatings with or without P.A. We used a Thermo-Nicolet Magna IR 760 spectrometer equipped with a Smart MIRacle ATR accessory with a diamond crystal. Spectra were collected over a range 500–4000 cm^{-1} with a resolution of 4 cm^{-1}. Each spectrum was produced by coaddition of 64 scans. Several identical specimens were tested for reproducibility.

2.2.3. Electrochemical impedance spectroscopy (EIS)

The coated aluminum Q-panels were conditioned in a vacuum desiccator at ageing temperature for 24 hours to ensure that they were dry before immersion and EIS tests. Coated panels were set in an electrochemical glass cell (Gamry) having a circular aperture with a silicon-rubber O-ring to get the tightness of the saline solution (NaCl 3%wt) used for the immersion tests. The assemblies were placed in ovens at different ageing temperatures (30°C,

40°C and 50°C). These ovens also act as a Faraday cage to limit external interferences on the system studied. For each temperature, we used several samples in order to obtain reproducible results. The water uptake was evaluated in situ using a two-electrode cell, in which an epoxy-coated aluminium Q-panel acts as the working electrode (exposed area was 12.5 cm^2) and a graphite rod as the counter electrode and pseudo-reference. EIS measurements were carried out using a Gamry REF 600+ at the open circuit potential (12 points per decade) in the 10 Hz-1 MHz frequency range. A 50 mV rms sinusoidal ac perturbation was chosen since a pure capacitive behavior was observed in the whole frequency range with no Faradic processes, as already reported in our previous work [21]. As the high frequency part of the impedance is completely dominated by the capacitive response of the coating [22,23], the coating capacitance (C_{HF}) was calculated at a fixed high frequency (f = 10 kHz) using the real (Z') and the imaginary (Z'') parts of the impedance, as shown in Eq. (1):

$$C_{HF} = \frac{-Z''}{2\pi \times f \times ((Z')^2 + (Z'')^2)} \quad (1)$$

The water uptake χ_v was then calculated from the Brasher and Kingsbury relation (Eq. 2) [24] using the capacitance at high frequency (C_{HF}):

$$\chi_v(\%) = \frac{\log(\frac{C_{HF}^t}{C_{HF}^0})}{\log(\varepsilon_w(T))} \times 100 \quad (2)$$

with C_{HF}^0 and C_{HF}^t the high frequency capacitance at t=0 (extrapolation at 0 of the first points of the curve $C_{HF} = f(t)$) and at time t, respectively, and $\varepsilon_w(T)$ the relative permittivity of water (depending on temperature, see Table 1) [25,26].

Table 1 *:* Relative permittivity of water depending on temperature

Temperature (°C)	30	40	50
ε_w	76.60	73.17	69.88

The Brasher and Kingsbury relation is known to give over-estimated water uptake values, as discussed in another paper [27]. In this previous work, we showed that it was possible to obtain water uptake values similar to those measured by gravimetry by introducing the time-dependant-thickness (measured by SECM [28]) into the Brasher and Kingsbury relation. This approach was also used in [21]. In the present paper, the coating swelling is not considered and the Brasher and Kingsbury relation is not modified because this data analysis erases the

temperature effect [21]. This allows to better evaluate the influence of ageing temperature onto water uptake process in coatings with or without physical ageing.

2.2.4. Blister test (BT)

The coated A-46 disc was inserted in the sample holder (stainless steel SS) and a screw-down crown was used to block the coated sample (Figure 1). AISI 316SS pipes (Swagelok) were connected to the sample holder and to the programmable syringe pump (KD Scientific). Sealing between the coated A-46 disc and the sample holder and between the sample holder and the pipes is ensured by O-rings. The stress was applied to the coating by injecting pressurized water on the rear face of the coated sample through a hole into the substrate that was drilled before application of the coating.

A pressure transducer allowed to measure pressure during the BT so the test results are given in the form of a pressure/volume or pressure/displacement evolution based. An USB microscope allowed to record videos/photographs during the BT.

In-house software (coded in Wolfram Mathematica) has been developed for controlling the pressure and displacement during blister testing of coatings. This software is designed to provide a simple and easy-to-use interface for controlling the test conditions and monitoring the results. Users can easily set and adjust the volume injected, the injected velocity and displacement parameters for the test, ensuring that the coating is subjected to the appropriate level of stress and that the results are accurate and reliable. The software also allows users to monitor the progress of the test in real-time, with clear visual indicators of the pressure and displacement readings.

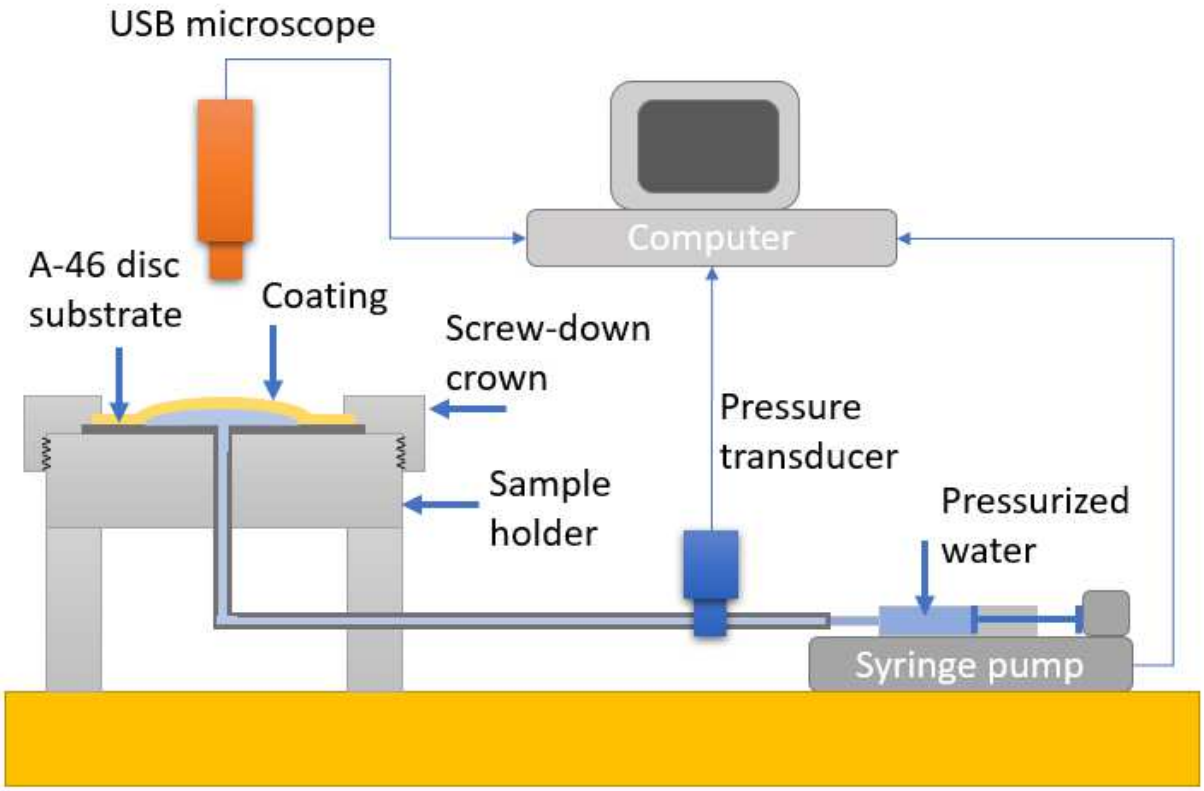

Fig. 1. Schematic of the blister test

3. Results and discussion

The initial part of this study aims to identify differences in initial properties between the systems with three different amounts of physical ageing (Tg, P.A. amount). The second part focuses on the effects of these differences on the water uptake and its diffusion in the coating network, and finally with the blister test to examine the question of adhesion.

3.1. Initial properties

The DGEBA/Jeffamine-230 coatings, obtained with the 3 different P.A. amounts were characterized by FTIR and DSC after their collection from the oven (at the dry state) before immersion tests. FTIR spectra from the pure DGEBA resin and from the DGEBA/Jeffamine-230 were compared (Figure 2a and 2b): the major bands are in agreement with the results reported in literature concerning epoxy systems [29–31] and clearly show the presence of absorption band around 914 cm^{-1} assigned to the vibration of the epoxide groups for the pure resin while it is not observed for the DGEBA/Jeffamine-230 system with no P.A. FTIR spectra obtained for the three DGEBA/Jeffamine230 networks were identical: typical

spectrum for the network with a maximum amount of P.A. is presented in Figure 2c and the subtraction results from spectrum b - spectrum c are presented in Figure 2d. As it can be seen, the subtraction results are close to 0 which means that there is no difference in IR bands. Finally, since no peak related to the epoxy group was observed in all DGEBA/Jeffamine230 spectra, it can be concluded that the networks are completely crosslinked and that no significant chemical change can be seen in FTIR spectra between networks with or without P.A.

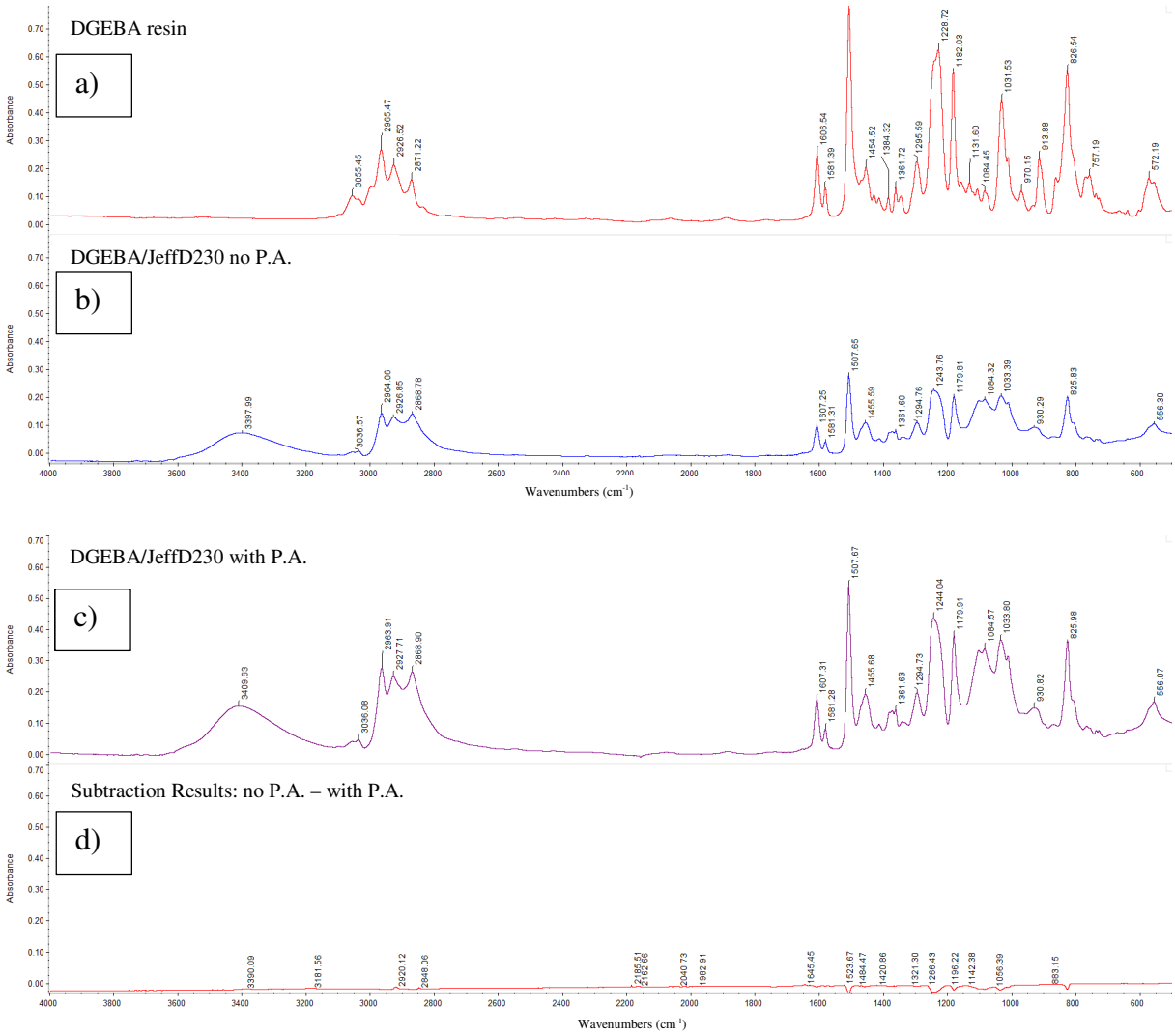

Fig. 2. Typical FTIR spectra for a) the pure DGEBA resin b) DGEBA/Jeffamine230 system without P.A. c) DGEBA/Jeffamine230 system with P.A. d) subtraction results for spectrum b – spectrum c.

Figure 3 presents the changes of the total heat flow for the 3 different systems. All samples show structural relaxation phenomenon (physical ageing [6]) of the resin after the curing cycle since there is appearance of an endothermic peak around Tg, with various magnitudes,

during the first DSC scan. It can be seen that, qualitatively, the magnitude of the endothermic peaks is apparently greater for the samples that were cooled at slower cooling rates (plateau of 76 hours at 73°C), followed by intermediate cooling rates (plateau of 1 hour at 88°C) and smaller for systems with a fast cooling. However, the presence of the endothermic peak makes difficult the evaluation of Tg or simply, impossible.

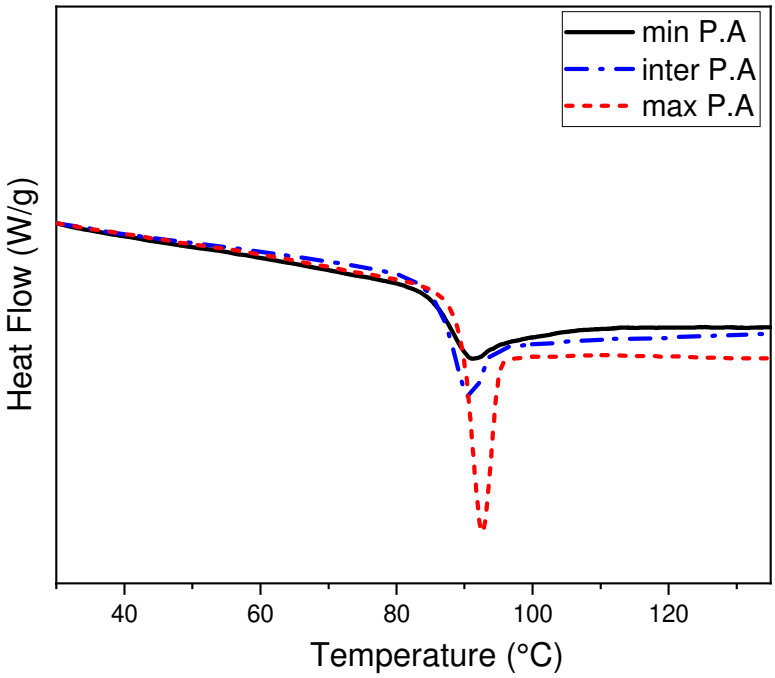

Fig. 3. DGEBA/Jeffamine-230 coating's DSC thermograms (first scan) for three different systems: minimum, intermediate and maximum of Physical Ageing.

The evaluation of Tg and the measurement of the physical ageing were then performed with the modulated mode of DSC (M-DSC). In this mode, the thermogram presents two signals: the reversing heat flux and the non-reversing heat flux. These two signals are result of deconvolution from the total enthalpy change (Heat Flow) [32]. Fig. 4 shows that Tg can be easily evaluated from the reversing heat flow signal (middle of transition) at about 91 °C for the 3 studied systems, with a minor increase in Tg with the structural relaxation [33,34]. The same value of Tg was achieved for the first and second scan, indicating that the system is completely cross-linked.

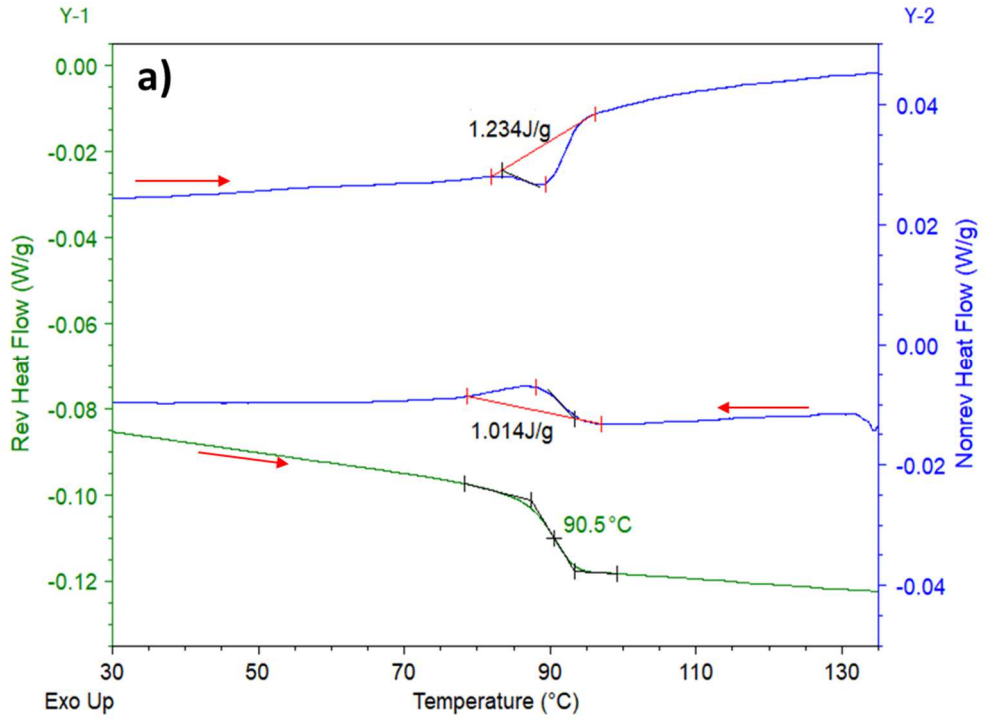
a)
Y-1
Y-2
1.234J/g
1.014J/g
90.5°C
Rev Heat Flow (W/g)
Nonrev Heat Flow (W/g)
Exo Up
Temperature (°C)

252

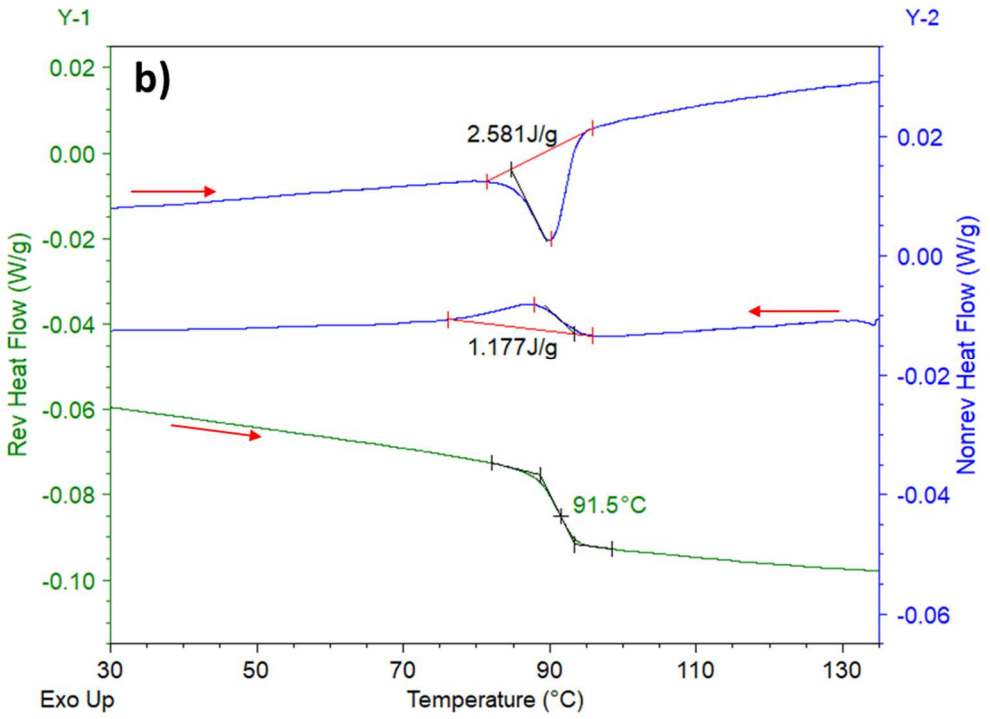
b)
Y-1
Y-2
2.581J/g
1.177J/g
91.5°C
Rev Heat Flow (W/g)
Nonrev Heat Flow (W/g)
Exo Up
Temperature (°C)

253

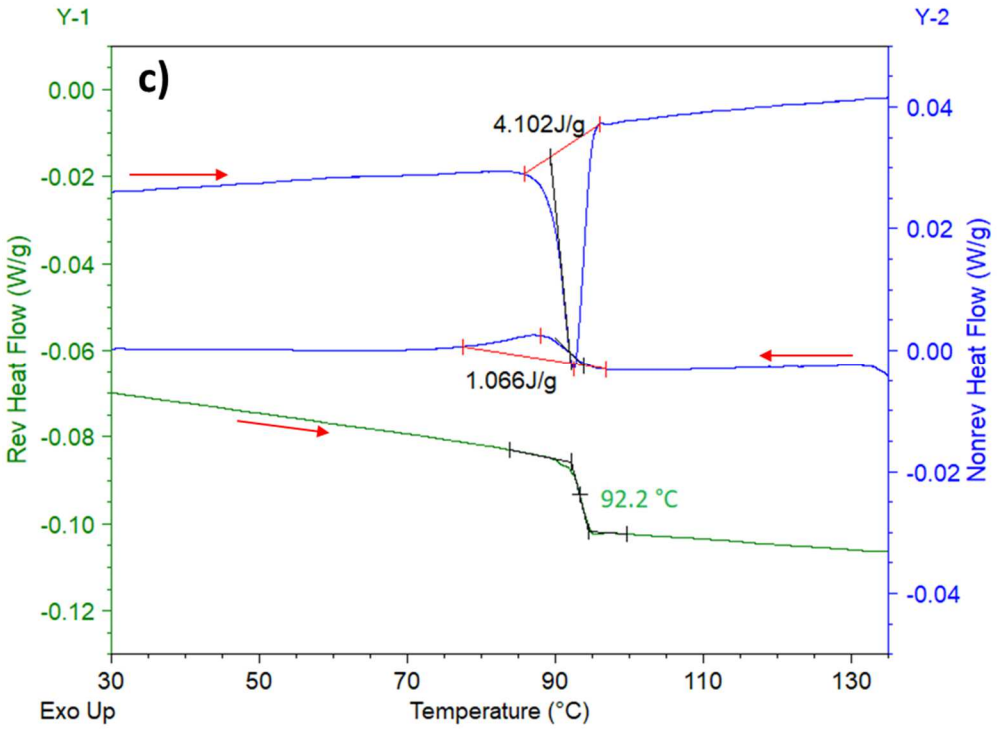

Fig. 4. Modulated DSC thermograms of the DGEBA/Jeffamine-230 coatings: a) minimum, b) intermediate and c) maximum of P.A

Physical ageing quantification is performed using the non-reversing heat flux signal. Two peaks are observed: an endothermic one during the temperature rise, characteristic of the P.A. and the stress frequency, and an exothermal one during the cooling, characteristic of only the stress frequency [35,36]. The difference in area between these two peaks indicates the excess of enthalpy due to structural relaxations present in the polymer network [37] and is called amount (or extent) of physical ageing [38–41]. The amount of P.A. and the Tg of the 3 studied systems are given in Table 2.

Table 2. Initial characteristics of the 3 studied systems of DGEBA/Jeffamine-230

	min P.A.	inter P.A.	max P.A.
Tg (°C)	90 ± 0.5	91 ± 1	92 ± 1
Amount of P.A. (J/g)	0.3 ± 0.1	1.3 ± 0.2	3.2 ± 0.1

A slow cooling allowed for a considerable amount of P.A. to be obtained. Indeed, the amount of physical ageing is dependent on the step of cooling and a slow cooling allows for more time for the polymer chains to rearrange themselves, leading to a greater degree of physical ageing. In contrast, a fast cooling rate to temperatures well below the Tg does not allow enough time for the polymer chains to rearrange, resulting in a lower degree of physical

ageing. The rapid cooling was supposed to avoid physical ageing, but in fact, we still manage to obtain some trace of P.A.

The interesting point is that controlling cooling step allows obtaining coatings with different amounts of physical ageing, without any chemical modification, as seen with FTIR results.

3.2. Sorption curves

Typical raw EIS curves are presented in Figure 5.a. As it can be seen, a pure capacitive behavior was obtained during the test period which means that the impedance is dominated by the coating response. Representative sorption curves obtained by EIS data using the Brasher and Kingsbury equation for the 3 different systems (min, inter and max of physical ageing) during immersion in NaCl 3 wt% solution at 30, 40 and 50 °C are presented in Fig. 5. In these curves, the evolution of water volume fraction (χ_v) is presented as function of the reduced time ($\boldsymbol{\tau} = t^{1/2}$ / thickness) in order to eliminate the thickness effect.

As it was seen previously [21], the volume water uptake measurements for all coated samples show a classical pseudo-Fickian behavior [5,42–44], with following features: for all systems, there is a rapid initial water absorption, followed by a slow water absorption and finally a plateau indicating water saturation. For all studied temperatures, systems with a minimum amount of P.A. have higher water uptake values at saturation than systems presenting maximum of P.A., with an intermediate system that takes place between the two values. Fig.6 points out the evolution of water uptake values χ_v (obtained from the Brasher and Kingsbury equation) at saturation with the ageing temperatures for the 3 different systems of P.A. It should be noticed that the same trends were observed with free films from gravimetry results (results not shown here).

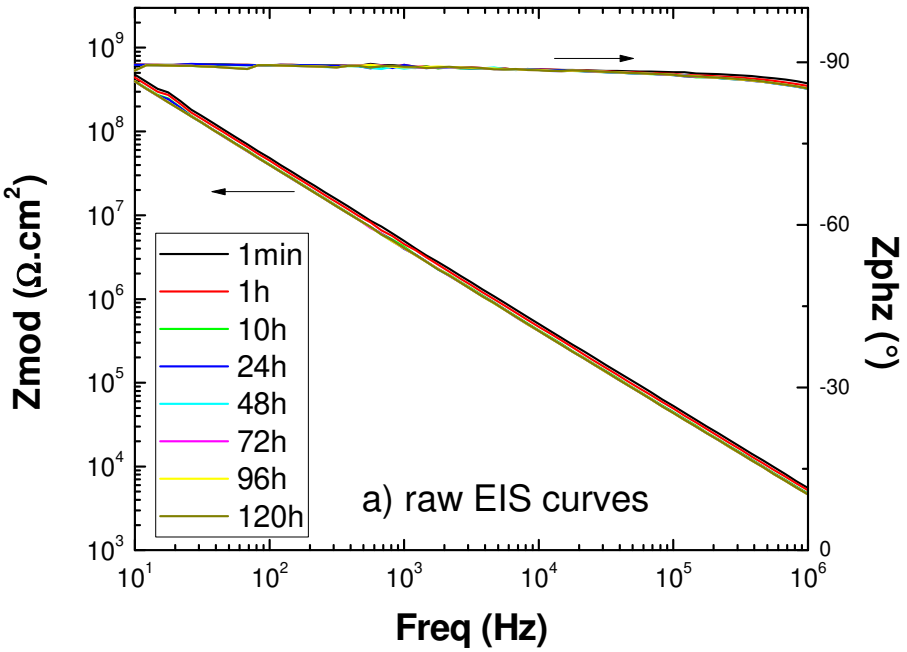
Zmod (Ω.cm²)
Zphz (°)
Freq (Hz)
1min
1h
10h
24h
48h
72h
96h
120h
a) raw EIS curves

293

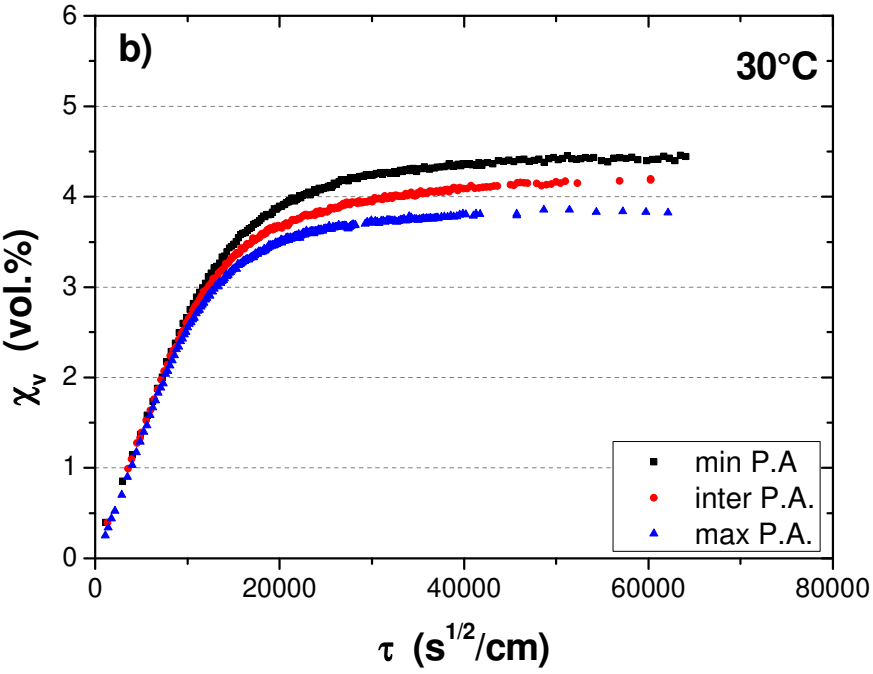
b)
30°C
χv (vol.%)
τ (s^1/2/cm)
min P.A
inter P.A.
max P.A.

294

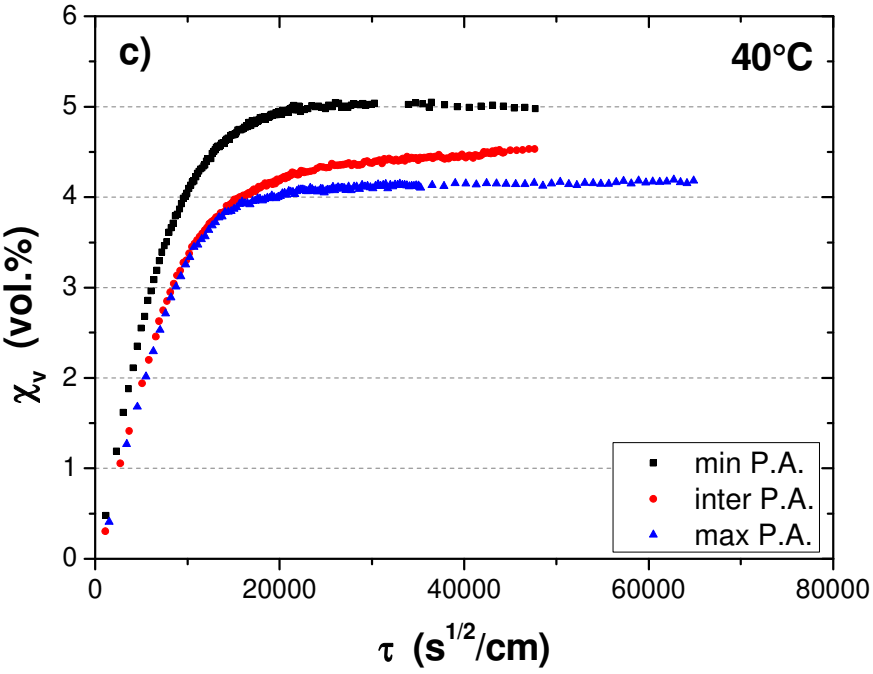

295

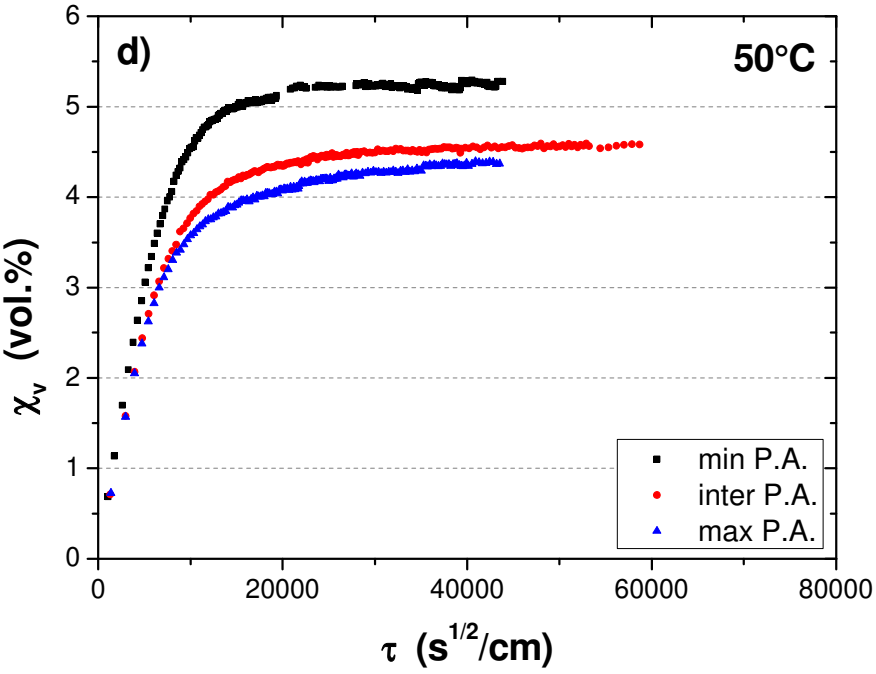

296

297 **Fig. 5.** Raw EIS curves for a coating without P.A. immersed at 30°C (a) and volume water uptake
298 curves for the 3 P.A. systems of coatings at different temperatures of immersion in NaCl 3 wt%: 30°C
299 (b), 40°C (c) and 50°C (d).

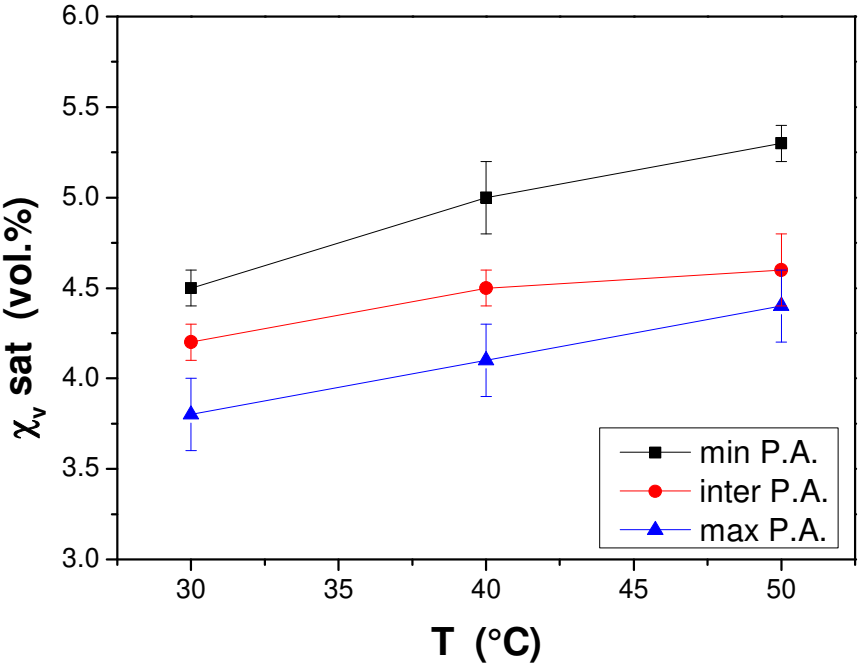

Fig. 6. Water uptake values at saturation (estimated from B&K equation) for the 3 different systems at 30, 40 and 50 °C

The increased water uptake in systems with low levels of P.A. can be attributed to a higher free volume fraction and reduced polymer chain interactions. Conversely, systems with high levels of P.A. exhibit a denser polymer network, leading to stronger polymer chain interactions and a lower free volume, which impede water penetration and decrease water uptake.

The low value of water uptake at 30 °C most likely owing to the lower number of attractive molecular segments that can be contacted since the mobility is greatly limited at low temperatures (distant from humid Tg=72 °C [21]). This is in line with what has been found previously about epoxy based resins by Akele et al. [11], Ding et al. [45], Starkova et al. [46], and more recently Gibhardt and al. [47].

3.3. Kinetics of diffusion

Since the water uptake mechanism in DGEBA/Jeffamine230 systems behave as a pseudo-Fickian diffusion profile, sorption curves are fitted using the dual Fick model, which takes into account two simultaneous diffusion processes, following Eq. (3) [48–50].

$$\chi_v(\tau) = \sum_{i=\{1,2\}} \left[{\chi_{v,i}}^{\infty} . \left(1 - \frac{8}{\pi^2} \sum_{n=0}^{\infty} \frac{1}{(2n+1)^2} . exp\left(\frac{-(2n+1)^2 . \pi^2 . D_i . \tau^2}{4} \right) \right) \right]$$

318 (3)

319 Where χ_v (τ) is the volume water uptake at the reduced time **τ**; $\chi_{v,i}^{\infty}$ is the water content at
320 saturation for diffusion process i (i=1,2) and D_i is the diffusion coefficient for diffusion
321 process i (i=1,2). Fig. 7 shows an example of fitting results for a coating with minimal P.A.
322 and another with maximal P.A. at 40 °C. The experimental curves (χ_v_exp) are fitted using
323 Eq. 3 (χ_v_$calc$) where $\chi_{v_{calc}} = \chi_{v,1} + \chi_{v,2}$.

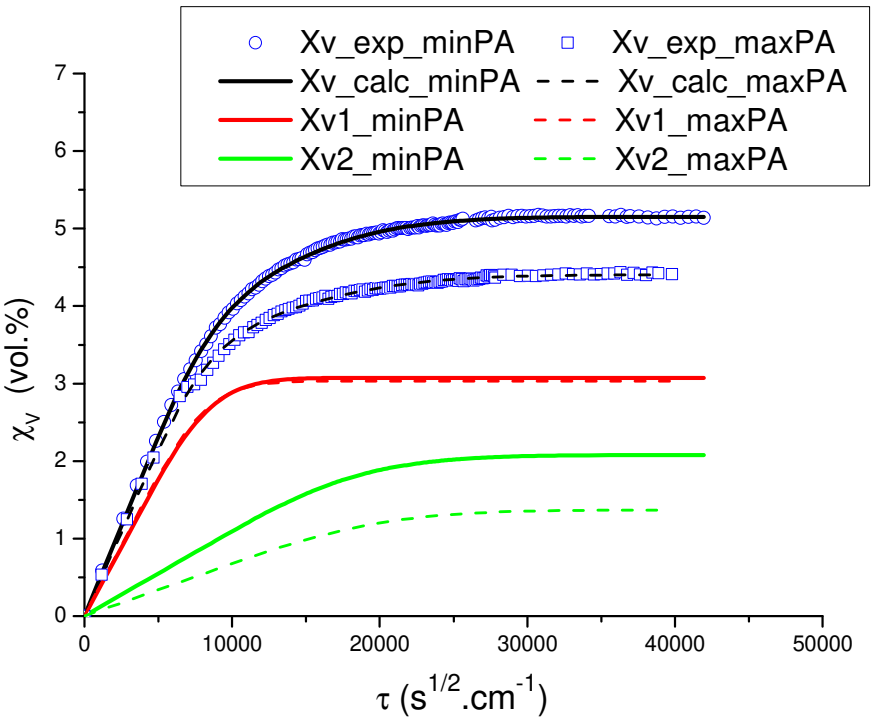

324

325 **Fig. 7.** Typical sorption curves (obtained from B&K Eq.2) fitted using a dual Fick Eq. (3) for 2
326 systems; minimum of P.A. and maximum of P.A. during immersion at 40 °C.

327 The initial diffusion process (corresponding to the diffusion coefficient D_1 in Fig. 7 and the
328 water saturation $\chi_{v,1}^{\infty}$) is characterized by the absorption of water by the polymer network,
329 which simultaneously leads to plasticization of the network. This plasticization and associated
330 swelling lead to an increase in the mobility of the polymer chains, facilitating the relaxation
331 and release of previously inaccessible polar sites. These newly available sites allow for further
332 water absorption, which constitutes the secondary diffusion process (corresponding to the
333 diffusion coefficient D_2 in Fig .7 and the water saturation $\chi_{v,2}^{\infty}$), resulting in a gradual
334 increase in the water uptake capacity of the polymer [14,16].

335 The values of the diffusion coefficients (D_1 & D_2) of water calculated thanks to Eq. (3), for all
336 studied systems, are presented in Table 3.

Table 3. Values of diffusion coefficients D_1 and D_2, calculated using Eq. (3), for coatings with minimum, intermediate and maximum of physical ageing at various ageing temperatures

	30 °C		40 °C		50 °C	
	D_1 (cm²/s)	D_2 (cm²/s)	D_1 (cm²/s)	D_2 (cm²/s)	D_1 (cm²/s)	D_2 (cm²/s)
min P.A.	$4.6\pm0.3\ 10^{-9}$	$8.3\pm0.2\ 10^{-10}$	$1.1\pm0.3\ 10^{-8}$	$2.8\pm0.5\ 10^{-9}$	$1.5\pm0.1\ 10^{-8}$	$3.3\pm0.3\ 10^{-9}$
inter P.A.	$4.8\pm0.4\ 10^{-9}$	$5.5\pm0.2\ 10^{-10}$	$9.4\pm0.2\ 10^{-9}$	$1.4\pm0.1\ 10^{-9}$	$1.6\pm0.4\ 10^{-8}$	$1.9\pm0.5\ 10^{-9}$
max P.A.	$5.0\pm0.4\ 10^{-9}$	$8.9\pm0.3\ 10^{-10}$	$8.4\pm0.1\ 10^{-9}$	$1.5\pm0.5\ 10^{-9}$	$1.5\pm0.4\ 10^{-8}$	$9.7\pm0.5\ 10^{-10}$

These results indicate a temperature-dependent behavior since both diffusion coefficients (D_1 and D_2) increase with the rise of temperature for the 3 studied systems (min, inter and max of P.A.), following an Arrhenius law characteristic of diffusion phenomena (Eq.4) [51]:

$$D_i = D_{0,i} \exp\left(-\frac{\Delta H_i}{RT}\right) \quad (4)$$

with i = 1 or 2, ΔH_i is the enthalpy of diffusion associated with the number of polar groups and the distance between two polar groups, $D_{0,i}$ is the pre-exponential factor for the diffusion coefficient, R is the ideal gas constant and T is the temperature.

To investigate the evolution of these coefficients with temperature and P.A., and furthermore to calculate the thermodynamic parameters of the diffusion, the natural logarithm of the values of Di (Ln (Di)) is plotted as a function of the inverse of the absolute temperature (Fig.8). A linear behavior of D_1 and D_2 (diffusion coefficients) with the inverse of the temperature (1/T) is observed and consequently the Arrhenius' law is verified. The estimation of $D_{0,i}$ and ΔH_i is allowed (Table 4).

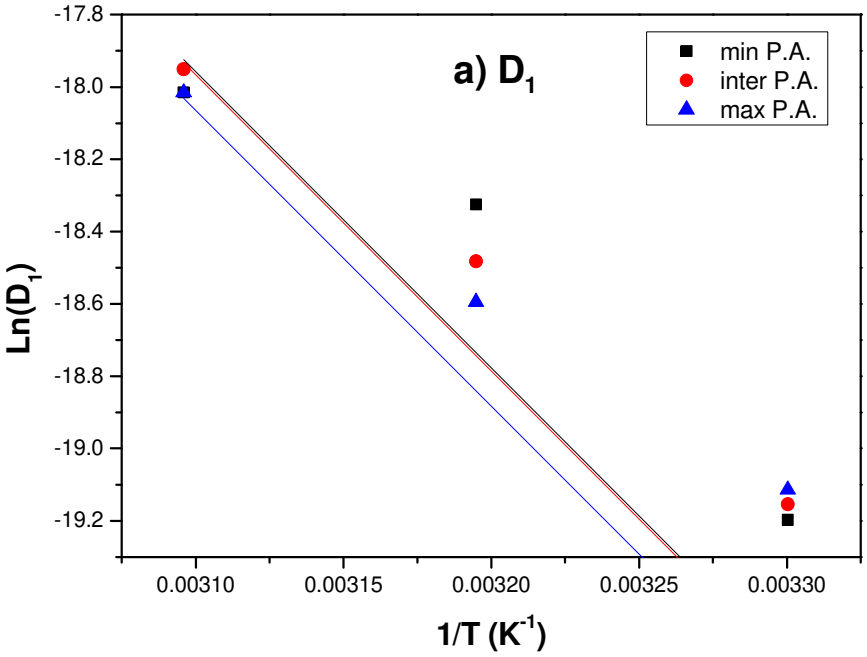

353

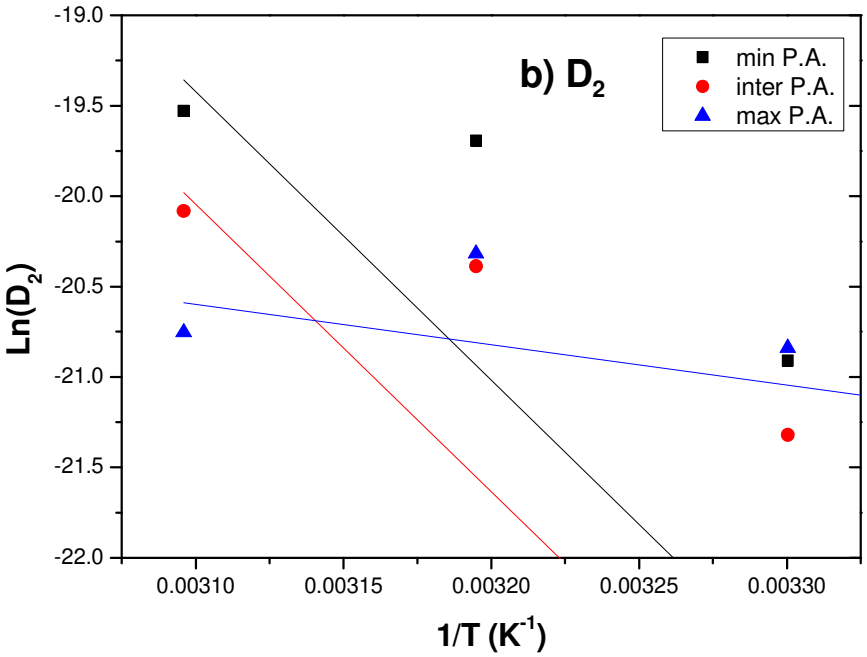

354

355 **Fig. 8.** Evolution of the diffusion coefficients D_1 (a) and D_2 (b) as a function of the inverse of the
356 temperature for the 3 studied systems (minimum, intermediate and maximum of P.A.)

357

D_1	D_2

	ΔH_1 (kJ/mol)	$D_{0,1}$ (cm²/s)	ΔH_2 (kJ/mol)	$D_{0,2}$ (cm²/s)
min P.A.	47	0.53	56	4.2
inter P.A.	50	1.7	49	0.28
max P.A.	44	0.17	44	5.1×10^{-9}

Table 4. Arrhenius' parameters applied to the D_1 and D_2 coefficients for the 3 studied systems

From Fig.8(a), similar slopes were identified for the first diffusion process (D_1). Furthermore, Table 4 confirms that for D_1, both ΔH and D_0, which correspond respectively to the enthalpy of diffusion of water molecules in the polymer matrix and to the number and variety of diffusion paths, are identical for all values of physical ageing. This means that the first diffusion process is thermally activated in the same way for all three amounts of P.A. Water diffuses and creates interactions with the macromolecular chains that are free to interact with it and which are not involved in the P.A. process. However, D_2 corresponds to the diffusion of water in the polymer matrix via polar sites which become accessible by relaxation due to plasticization and swelling (Fig.8 (b)). For higher P.A. values, these thermodynamic parameters appear to be lower. The physical ageing leads to a densification of the network. The macromolecular chains move closer to each other, resulting in the creation and or reinforcement of polymer/polymer bonds and a reduction in the free volume. A diffusing water molecule can then more simply reach another polar group of polymer by making a less energy transition and also fewer diffusing pathways are possible [14,21,47]. In other words, the higher the physical ageing, the less the second diffusion is thermally activated, the interacting macromolecular chains are prevented from relaxing by the physical ageing and cannot contribute to the water diffusion (Fig.9).

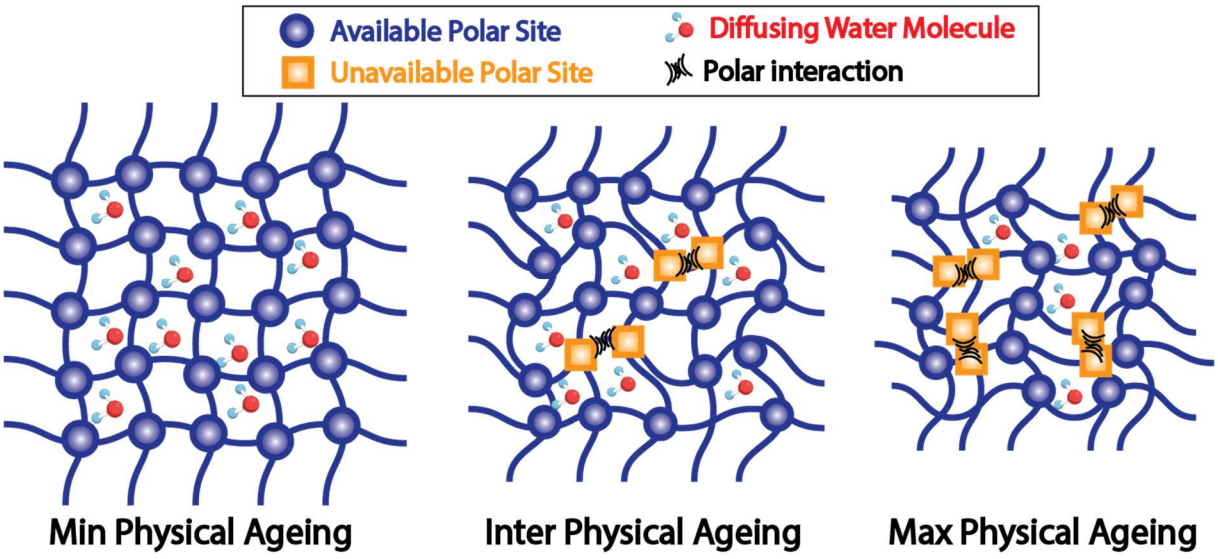

Fig. 9. Schema describing the influence of physical ageing of a diffusing water in polymer network.

3.4. Blister test

Results were obtained using the blister test (BT) at a constant liquid flow rate of 350 µL/min and a sticker of 24 mm, between the substrate and the coating as a blister initiator. At least three identical samples were tested for reproducibility. As seen previously, the systems with a minimum amount of P.A. and a maximum amount of P.A. present the largest differences. Therefore, only these specimens with min and max P.A. are considered in this part.

Figure 10 presents the pressure vs. the injected volume for the dry systems. It can be clearly seen that during the BT experiment, and for both systems (min P.A. and max P.A.), the pressure increased continuously until the detachment of the coating at the blister initiator (removal of the sticker) and then it continued to increase until a critical pressure (Pc) where the coating fails.

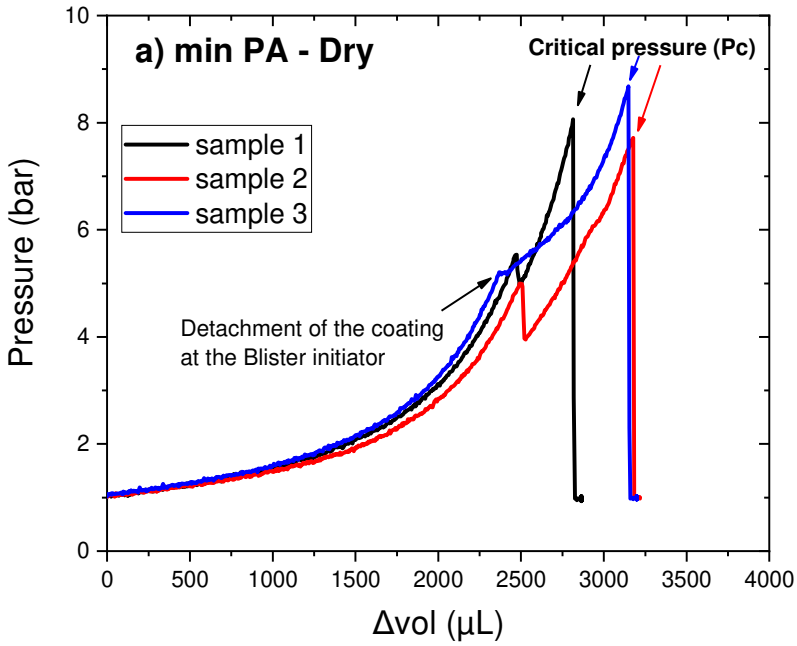

392

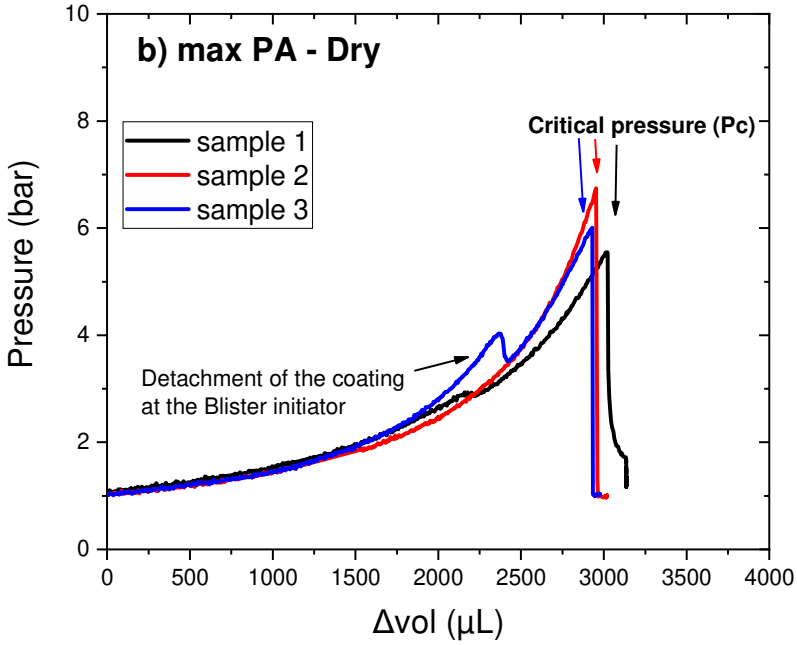

393

394 **Fig. 10.** Blister test data in form of pressure versus injected volume for dry samples with a) min P.A.
395 and b) max P.A.

396

397 Fig.11 shows the dry coating with min P.A. before and after the BT, thanks to the
398 photographs recorded by the USB microscope. It can be easily noticed that the failure of the
399 coating was at the level of the sticker without any propagation of the blister. This cohesive

failure can be due to the fact that our system is very rigid and brittle so the coating cannot elastically deform a lot with the applied stress. The same behavior is observed for the dry coating with a max P.A.

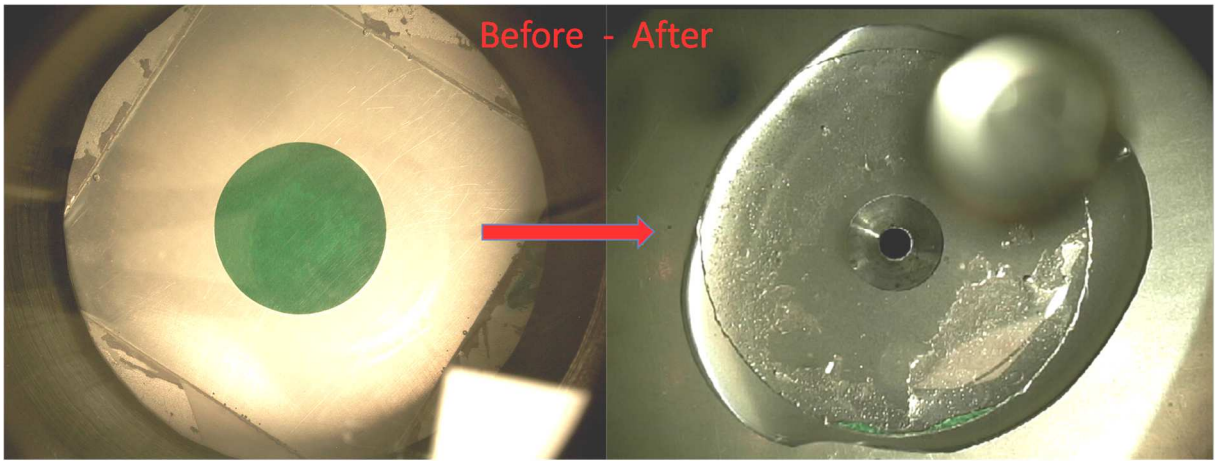

Fig. 11. Photographs recorded by the USB microscope for a dry sample with min P.A.

Fig. 12 shows the evolution of pressure as a function of injected volume for samples saturated in water at 40 °C. The critical pressure was very low comparing to the dry samples and a blister propagation can be observed after the critical pressure for both systems (min and max P.A.). Fig. 13 confirms the adhesive failure and shows the delamination of the coating film caused by water propagation. The low values of Pc, for saturated samples, are due to plasticization and swelling of the polymer, which reduce the rigidity of the coating and thus allow a larger deformation of the coating and the appearance of a blister.

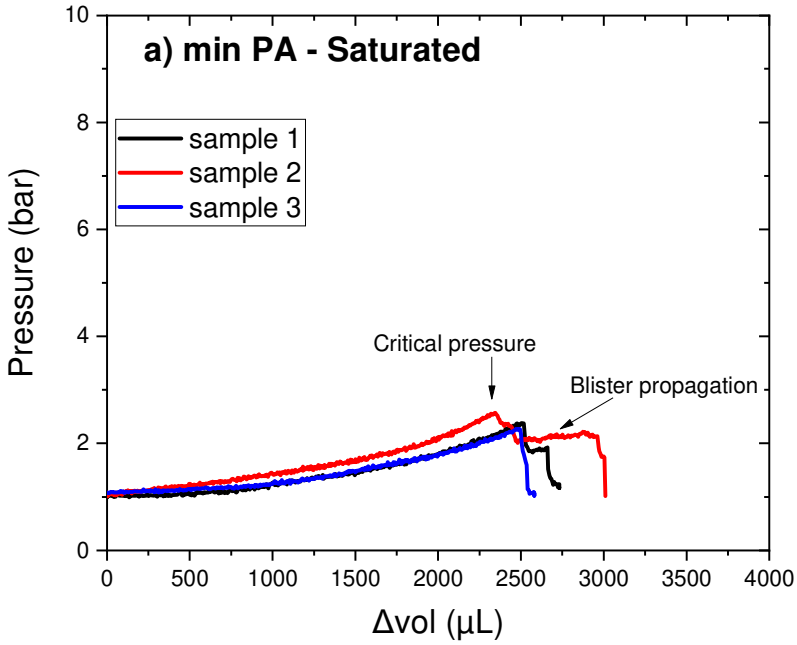

413

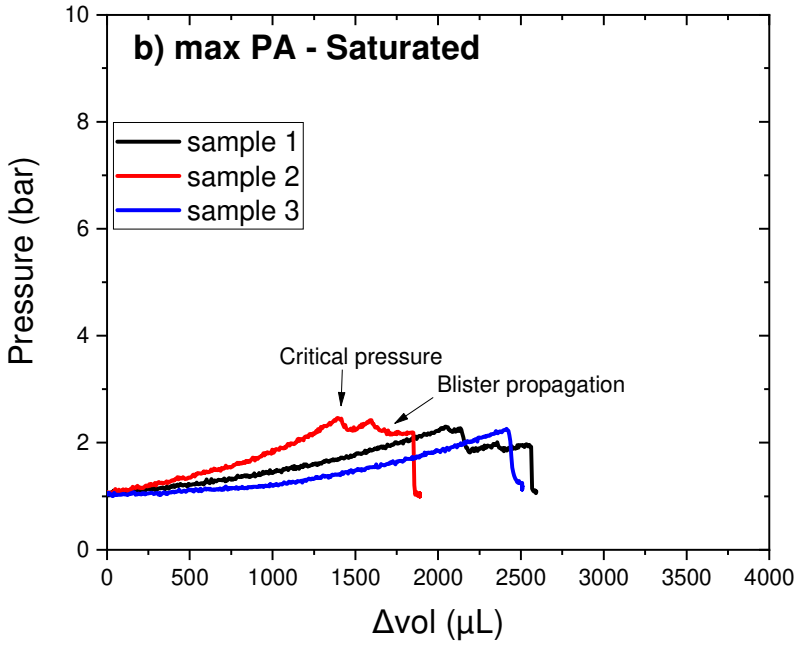

414

415 **Fig. 12.** Blister test data in form of pressure versus injected volume for saturated samples at 40 °C
416 with a) min P.A. and b) max P.A.

417

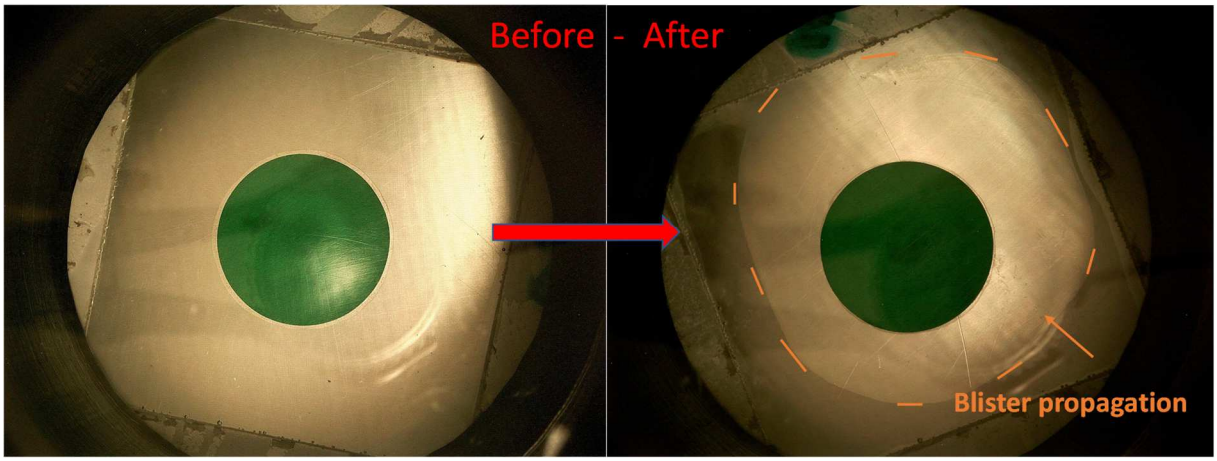

Fig. 13. Photographs recorded by the USB microscope for a saturated sample with min P.A.

The average values of the critical pressure (Pc) were taken from graphs and are presented in Table 5. An important difference between Pc values for dry and saturated coatings for both systems (min and max P.A.) is observed. According to Gent and Schult [52] the work of detachment is decreased in the presence of a wetting liquid at the coating/substrate interface. Moreover, comparing Pc values for min and max P.A., the difference is only observed for the dry state. With max P.A., the network is denser and so, more rigid. Higher Pc values should be obtained. However, the strain is localized at the cracking point where the stress concentration is more important. This leads to a premature cohesive failure of the coating with max P.A. instead of an adhesive failure for lower Pc values.

Table 5. The average values of the critical pressure (Pc) for all studied systems

	Dry	Saturated
min P.A.	8.1 bars	2.4 bars
max P.A.	6.1 bars	2.3 bars

Future work using the blister test might focus on the quantitative effect of physical ageing and water uptake on the adhesion of epoxy coatings, using the critical pressure Pc to calculate the strength energy of adhesion.

4. Conclusion

In this work, DGEBA/Jeffamine230 epoxy coatings were obtained with three different amounts of physical ageing thanks to adapted cooling processes. Then, they were immersed in a saline solution to determine water uptake characteristics using EIS and they were submitted to the blister test to evaluate the effect of physical ageing onto adhesion properties.

Initial characterization of the coatings by FTIR showed that the different systems present identical chemical behaviors, so physical ageing does not significantly affect the chemical properties. Modulated DSC results showed a slight Tg increase (+1°C) with physical ageing which can be explained by the structural relaxation induced by P.A., leading to a denser network and higher Tg. During immersion in the saline solution at different ageing temperatures, the water uptake values at saturation were found to be lower with maximum amount of physical ageing. This was explained by a denser polymer network in the case of physical ageing that leads simultaneously to an increase of the polymer chain interactions and a decrease of the free volume, both impeding water uptake values.

Analysis of water diffusion within the three physically-aged networks showed a dual-Fick behavior, indicating that two different diffusion processes had to be considered. The first one is due to the initial water ingress that leads to the polymer plasticization and the release of new polar sites that become available for water diffusion in a second step, when polymer chains are relaxed. However, this relaxation process is lower in case of physical ageing because of stronger interactions between polymer chains.

The adhesion of physically-aged coatings was evaluated by the blister test, before and after immersion at 40 °C. The critical pressure needed for the coating failure was found to be higher for dry systems and for lower values of physical ageing. Cohesive failures were obtained for dry systems because the DGEBA/Jeffamine230 is rigid and can not deform. When the systems are water saturated, the critical pressure is much lower, with or without physical ageing. From all these results, it seems that adhesion is mainly governed by the presence of water at the coating interface and the physical ageing only delays the arrival of water at the metallic substrate.

The results of this study demonstrate the importance of considering the physical ageing and the impact of water absorption in evaluating the service life of organic coatings in real-world applications.

Declarations

Funding

Authors would like to thank the Region Nouvelle-Aquitaine (France) for PhD financing.

Conflicts of interest

The Authors declare that there is no conflict of interest.

Availability of data and material

Not applicable

Code availability

Not applicable

References

[1] O. Negele, W. Funke, Internal stress and wet adhesion of organic coatings, Progress in Organic Coatings. 28 (1996) 285–289. https://doi.org/10.1016/0300-9440(95)00606-0.

[2] F. Mansfeld, H. Xiao, L.T. Han, C.C. Lee, Electrochemical impedance and noise data for polymer coated steel exposed at remote marine test sites, Progress in Organic Coatings. 30 (1997) 89–100. https://doi.org/10.1016/S0300-9440(96)00675-3.

[3] F. Deflorian, S. Rossi, An EIS study of ion diffusion through organic coatings, Electrochimica Acta. 51 (2006) 1736–1744. https://doi.org/10.1016/j.electacta.2005.02.145.

[4] G.K. van der Wel, O.C.G. Adan, Moisture in organic coatings — a review, Progress in Organic Coatings. 37 (1999) 1–14. https://doi.org/10.1016/S0300-9440(99)00058-2.

[5] D. Nguyen Dang, B. Peraudeau, S. Cohendoz, S. Mallarino, X. Feaugas, S. Touzain, Effect of mechanical stresses on epoxy coating ageing approached by Electrochemical Impedance Spectroscopy measurements, Electrochimica Acta. 124 (2014) 80–89. https://doi.org/10.1016/j.electacta.2013.08.111.

[6] E.C.L. Struik, Physical aging in amorphous polymers and other materials, PhD thesis, Delft university, 1977.

[7] L.C.E. Struik, Physical aging in plastics and other glassy materials, Polymer Engineering & Science. 17 (1977) 165–173. https://doi.org/10.1002/pen.760170305.

[8] L.C.E. Struik, Physical Aging in Amorphous Glassy Polymers, Annals of the New York Academy of Sciences. 279 (1976) 78–85. https://doi.org/10.1111/j.1749-6632.1976.tb39695.x.

[9] G.M. Odegard, A. Bandyopadhyay, Physical aging of epoxy polymers and their composites, J. Polym. Sci. B Polym. Phys. 49 (2011) 1695–1716. https://doi.org/10.1002/polb.22384.

[10] E.S.-W. Kong, Physical aging in epoxy matrices and composites, in: K. Dušek (Ed.), Epoxy Resins and Composites IV, Springer Berlin Heidelberg, Berlin, Heidelberg, 1986: pp. 125–171. https://doi.org/10.1007/3-540-16423-5_14.

[11] N. Akele, F. Thominette, D. Paris, M.F. Pays, J. Verdu, Physical ageing and water sorption in polycarbonate, J Mater Sci Lett. 15 (1996) 1001–1002. https://doi.org/10.1007/BF00241449.

[12] V. Bellenger, J. Verdu, E. Morel, Structure-properties relationships for densely cross-linked epoxide-amine systems based on epoxide or amine mixtures, J Mater Sci. 24 (1989) 63–68. https://doi.org/10.1007/BF00660933.

[13] X. Colin, Nonempirical Kinetic Modeling of Non-fickian Water Absorption Induced by a Chemical Reaction in Epoxy-Amine Networks, in: P. Davies, Y.D.S. Rajapakse (Eds.), Durability of Composites in a Marine Environment 2, Springer International Publishing, Cham, 2018: pp. 1–18. https://doi.org/10.1007/978-3-319-65145-3_1.

[14] G. Bouvet, N. Dang, S. Cohendoz, X. Feaugas, S. Mallarino, S. Touzain, Impact of polar groups concentration and free volume on water sorption in model epoxy free films and coatings, Progress in Organic Coatings. 96 (2016) 32–41. https://doi.org/10.1016/j.porgcoat.2015.12.011.

[15] O. Starkova, S. Chandrasekaran, T. Schnoor, J. Sevcenko, K. Schulte, Anomalous water diffusion in epoxy/carbon nanoparticle composites, Polymer Degradation and Stability. 164 (2019) 127–135. https://doi.org/10.1016/j.polymdegradstab.2019.04.010.

[16] A. Le Guen-Geffroy, P.-Y. Le Gac, B. Habert, P. Davies, Physical ageing of epoxy in a wet environment: Coupling between plasticization and physical ageing, Polymer Degradation and Stability. 168 (2019) 108947. https://doi.org/10.1016/j.polymdegradstab.2019.108947.

[17] A. Le Guen-Geffroy, P. Davies, P.-Y. Le Gac, B. Habert, Influence of Seawater Ageing on Fracture of Carbon Fiber Reinforced Epoxy Composites for Ocean Engineering, Oceans. 1 (2020) 198–214. https://doi.org/10.3390/oceans1040015.
[18] B.C. Rincon Troconis, G.S. Frankel, Effect of Roughness and Surface Topography on Adhesion of PVB to AA2024-T3 using the Blister Test, Surface and Coatings Technology. 236 (2013) 531–539. https://doi.org/10.1016/j.surfcoat.2013.10.046.
[19] H. Dannenberg, Measurement of adhesion by a blister method, J. Appl. Polym. Sci. 5 (1961) 125–134. https://doi.org/10.1002/app.1961.070051401.
[20] M. Arrigoni, S. Barradas, M. Braccini, M. Dupeux, M. Jeandin, M. Boustie, C. Bolis, L. Berthe, A comparative study of three adhesion tests (EN 582, similar to ASTM C633, LASAT (LASer Adhesion Test), and bulge and blister test) performed on plasma sprayed copper deposited on aluminium 2017 substrates, Journal of Adhesion Science and Technology. 20 (2006) 471–487. https://doi.org/10.1163/156856106777144336.
[21] Y. Elkebir, S. Mallarino, D. Trinh, S. Touzain, Effect of physical ageing onto the water uptake in epoxy coatings, Electrochimica Acta. 337 (2020) 135766. https://doi.org/10.1016/j.electacta.2020.135766.
[22] S. Duval, M. Keddam, M. Sfaira, A. Srhiri, H. Takenouti, Electrochemical Impedance Spectroscopy of Epoxy-Vinyl Coating in Aqueous Medium Analyzed by Dipolar Relaxation of Polymer, J. Electrochem. Soc. 149 (2002) B520. https://doi.org/10.1149/1.1512667.
[23] A.S. Castela, A.M. Simões, Water sorption in freestanding PVC films by capacitance measurements, Progress in Organic Coatings. 46 (2003) 130–134. https://doi.org/10.1016/S0300-9440(02)00220-5.
[24] D.M. Brasher, A.H. Kingsbury, Electrical measurements in the study of immersed paint coatings on metal. I. Comparison between capacitance and gravimetric methods of estimating water-uptake, J. Appl. Chem. 4 (1954) 62–72. https://doi.org/10.1002/jctb.5010040202.
[25] D.R. Lide, CRC Handbook of Chemistry and Physics, 85th Edition, 75th edition, CRC Press, 1994.
[26] C.G. Malmberg, A.A. Maryott, Dielectric constant of water from 0 to 100 C, J. Res. Natl. Bur. Stan. 56 (1956) 1. https://doi.org/10.6028/jres.056.001.
[27] C. Vosgien Lacombre, G. Bouvet, D. Trinh, S. Mallarino, S. Touzain, Water uptake in free films and coatings using the Brasher and Kingsbury equation: a possible explanation of the different values obtained by electrochemical Impedance spectroscopy and gravimetry, Electrochimica Acta. 231 (2017) 162–170. https://doi.org/10.1016/j.electacta.2017.02.051.
[28] G. Bouvet, T. Dao, S. Mallarino, X. Feaugas, S. Touzain, In situ monitoring of organic coating swelling by dynamic mechanical analysis and scanning electrochemical microscopy, Progress in Organic Coatings. 96 (2016) 13–18. http://dx.doi.org/10.1016/j.porgcoat.2016.01.026.
[29] Y. Malajati, Etude des mécanismes de photovieillissement de revêtements organiques anti-corrosion pour application comme peintures marines. Influence de l'eau, Université Blaise Pascal, 2009. https://tel.archives-ouvertes.fr/tel-00725456/document.
[30] Y. Ngono, Y. Maréchal, N. Mermilliod, Epoxy−Amine Reticulates Observed by Infrared Spectrometry. I: Hydration Process and Interaction Configurations of Embedded H2O Molecules, J. Phys. Chem. B. 103 (1999) 4979–4985. https://doi.org/10.1021/jp984809y.
[31] Y. Ngono, Y. Maréchal, Epoxy–amine reticulates observed by infrared spectrometry. III. Modifications of the structure and hydration abilities after irradiation in a humid atmosphere, Journal of Polymer Science Part B: Polymer Physics. 39 (2001) 1129–1136. https://doi.org/10.1002/polb.1089.

576 [32] M. Reading, A. Luget, R. Wilson, Modulated differential scanning calorimetry,
577 Thermochimica Acta. 238 (1994) 295–307. https://doi.org/10.1016/S0040-
578 6031(94)85215-4.
579 [33] C.T. Moynihan, Phenomenology of the structural relaxation process and the glass
580 transition, in: ASTM Special Technical Publication, 1249, 1994: pp. 32–49.
581 [34] A. Roggero, L. Villareal, N. Caussé, A. Santos, N. Pébère, Correlation between the
582 physical structure of a commercially formulated epoxy paint and its electrochemical
583 impedance response, Progress in Organic Coatings. 146 (2020) 105729.
584 https://doi.org/10.1016/j.porgcoat.2020.105729.
585 [35] D.J. Hourston, M. Song, A. Hammiche, H.M. Pollock, M. Reading, Modulated
586 differential scanning calorimetry: 2. Studies of physical ageing in polystyrene, Polymer.
587 37 (1996) 243–247. https://doi.org/10.1016/0032-3861(96)81094-9.
588 [36] D.J. Hourston, M. Song, H.M. Pollock, A. Hammiche, Modulated differential scanning
589 calorimetry : III. Applications to measurements of the glass transition temperature and
590 increment of heat capacity, Journal of Thermal Analysis. 49 (1997) 209–2018.
591 [37] M. Song, Modulated Differential Scanning Calorimetry Observation of Physical Ageing
592 in Polymers, Journal of Thermal Analysis and Calorimetry,. 63 (2001) 699–707.
593 [38] D.S. Matsumoto, Time-temperature superposition and physical aging in amorphous
594 polymers, Polymer Engineering & Science. 28 (1988) 1313–1317.
595 https://doi.org/10.1002/pen.760282005.
596 [39] S.G. Croll, X. Shi, B.M.D. Fernando, The interplay of physical aging and degradation
597 during weathering for two crosslinked coatings, Progress in Organic Coatings. 61 (2008)
598 136–144. https://doi.org/10.1016/j.porgcoat.2007.09.024.
599 [40] T. Sakai, T. Tao, S. Somiya, Viscoelasticity of Shape Memory Polymer: Polyurethane
600 series DiARY, Journal of Solid Mechanics and Materials Engineering. 1 (2007) 480–
601 489. https://doi.org/10.1299/jmmp.1.480.
602 [41] J.N. Hay, The physical ageing of amorphous and crystalline polymers, Pure and Applied
603 Chemistry. 67 (1995) 1855–1858. https://doi.org/10.1351/pac199567111855.
604 [42] A.R. Berens, H.B. Hopfenberg, Diffusion and relaxation in glassy polymer powders: 2.
605 Separation of diffusion and relaxation parameters, Polymer. 19 (1978) 489–496.
606 https://doi.org/10.1016/0032-3861(78)90269-0.
607 [43] M.M. Wind, H.J.W. Lenderink, A capacitance study of pseudo-fickian diffusion in
608 glassy polymer coatings, Progress in Organic Coatings. 28 (1996) 239–250.
609 https://doi.org/10.1016/0300-9440(95)00601-X.
610 [44] E.M. Davis, M. Minelli, M. Giacinti Baschetti, Y.A. Elabd, Non-Fickian Diffusion of
611 Water in Polylactide, Ind. Eng. Chem. Res. 52 (2013) 8664–8673.
612 https://doi.org/10.1021/ie302342m.
613 [45] Y. Ding, M. Liu, S. Li, S. Zhang, W.-F. Zhou, B. Wang, Contributions of the Side
614 Groups to the Characteristics of Water Absorption in Cured Epoxy Resins,
615 Macromolecular Chemistry and Physics. 202 (2001) 2681–2685.
616 https://doi.org/10.1002/1521-3935(20010901)202:13<2681::AID-
617 MACP2681>3.0.CO;2-E.
618 [46] O. Starkova, S.T. Buschhorn, E. Mannov, K. Schulte, A. Aniskevich, Water transport in
619 epoxy/MWCNT composites, European Polymer Journal. 49 (2013) 2138–2148.
620 https://doi.org/10.1016/j.eurpolymj.2013.05.010.
621 [47] D. Gibhardt, C. Buggisch, D. Meyer, B. Fiedler, Hygrothermal Aging History of Amine-
622 Epoxy Resins: Effects on Thermo-Mechanical Properties, Front. Mater. 9 (2022)
623 826076. https://doi.org/10.3389/fmats.2022.826076.
624 [48] W.K. Loh, A.D. Crocombe, M.M. Abdel Wahab, I.A. Ashcroft, Modelling anomalous
625 moisture uptake, swelling and thermal characteristics of a rubber toughened epoxy

626 adhesive, International Journal of Adhesion and Adhesives. 25 (2005) 1–12.
627 https://doi.org/10.1016/j.ijadhadh.2004.02.002.
628 [49] M.D. Placette, X. Fan, Jie-Hua Zhao, D. Edwards, A dual stage model of anomalous
629 moisture diffusion and desorption in epoxy mold compounds, in: 2011 12th Intl. Conf.
630 on Thermal, Mechanical & Multi-Physics Simulation and Experiments in
631 Microelectronics and Microsystems, IEEE, Linz, Austria, 2011: p. 1/8-8/8.
632 https://doi.org/10.1109/ESIME.2011.5765824.
633 [50] J. Cocaud, A. Célino, S. Fréour, F. Jacquemin, What about the relevance of the diffusion
634 parameters identified in the case of incomplete Fickian and non-Fickian kinetics?,
635 Journal of Composite Materials. 53 (2019) 1555–1565.
636 https://doi.org/10.1177/0021998318805823.
637 [51] M. Huldén, C.M. Hansen, Water permeation in coatings, Progress in Organic Coatings.
638 13 (1985) 171–194. https://doi.org/10.1016/0033-0655(85)80025-X.
639 [52] A.N. Gent, J. Schultz, Effect of Wetting Liquids on the Strength of Adhesion of
640 Viscoelastic Material, The Journal of Adhesion. 3 (1972) 281–294.
641 https://doi.org/10.1080/00218467208072199.
642

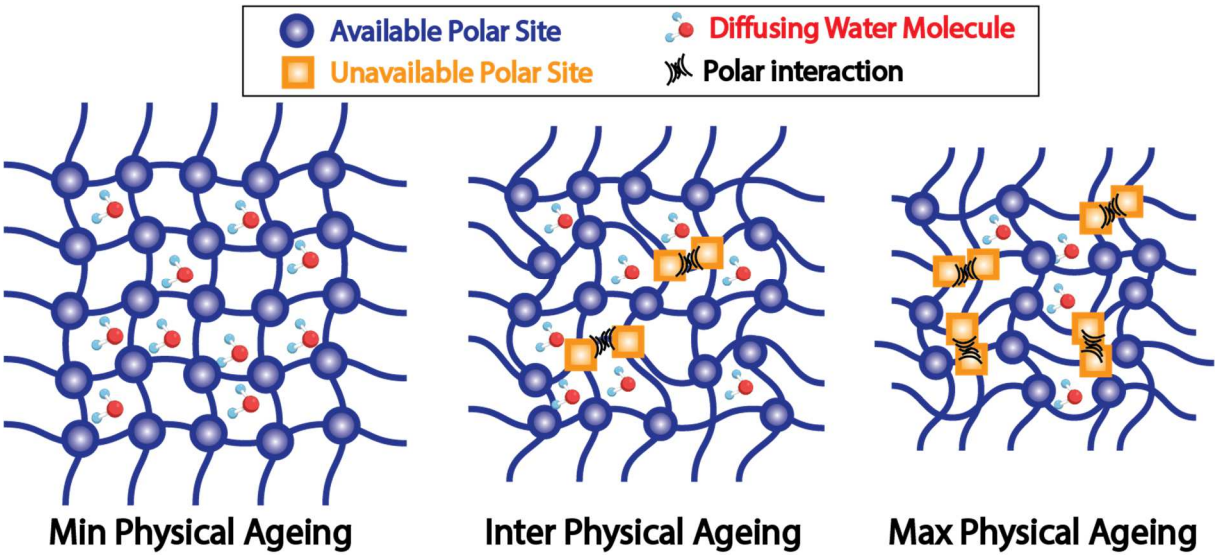
Available Polar Site
Unavailable Polar Site
Diffusing Water Molecule
Polar interaction
Min Physical Ageing
Inter Physical Ageing
Max Physical Ageing